SURFACE ENHANCED RAMAN SPECTROSCOPY ON DIELECTROPHORESIS INDUCED DIFFUSION LIMITED AGGREGATION OF GOLD NANOPARTICLES

by

Faisal Khair Chowdhury

A thesis submitted to the faculty of
The University of Utah
in partial fulfillment of the requirements for the degree of

Master of Science

Department of Electrical and Computer Engineering

The University of Utah

May 2011

The University of Utah Graduate School

STATEMENT OF THESIS APPROVAL

The thesis of **Faisal Khair Chowdhury**

has been approved by the following supervisory committee members:

Massood Tabib-Azar	, Chair	**3/1/2011** Date Approved
Behrouz Farang	, Member	**3/1/2011** Date Approved
Rajesh Menon	, Member	**3/1/2011** Date Approved

and by **Gianluca Lazzi** , Chair of

the Department of **Electrical and Computer Engineering**

and by Charles A. Wight, Dean of The Graduate School.

ABSTRACT

Wires formed by diffusion limited aggregation (DLA) induced by dielectrophoresis (DEP) of gold nanoparticles were investigated as an effective sample preparation method for surface enhanced Raman spectroscopy (SERS). Thymine was used as a test molecule and its SERS was measured to investigate the effectiveness of this technique that reproducibly resulted in $x10^9$ enhancement. It is known that molecules adsorbed near or at the surface of certain nanostructures produce strongly increased Raman signals and such phenomena is attributed to the concentration of electromagnetic (EM) optical fields at "hotspots" that usually occur at nanoscale junctions or clefts in metal nanostructures. Similarly, the enhancement obtained is attributed to the localized surface Plasmon's of the gold nanoparticles and the formation of "hotspots" in DEP wires. There are other methods that reproducibly yield in excess of $x10^8$ enhancement in SERS using tunable lasers and very elaborate Raman spectroscopy. The results presented here are obtained using a fixed laser excitation source at 785 nm and a simple spectrometer (5 cm^{-1} resolution).

This thesis is dedicated to my loving family, particularly, my sisters, brother and friends who have supported me throughout the course of my research.

Moreover, this thesis is especially dedicated to my dearly loved fiancée who taught me that everything is possible and most importantly, to believe in myself.

TABLE OF CONTENTS

LIST OF FIGURES

LIST OF TABLES

Table Page

ACKNOWLEDGEMENTS

I would like to thank all the people who have helped and inspired me during my project and thesis research. I especially want to thank my advisor, Prof. Massood Tabib-Azar, for his encouragement, guidance and support during my research and study at the University of Utah. His perpetual energy and enthusiasm in research has always motivated me to achieve better. In addition, he was always accessible and willing to help his students with their research. As a result, my research advanced speedily, smoothly and was very rewarding for me. In addition, I offer my deepest gratitude to the members of my supervisory committee, Dr. Behrouz Farhang-Boroujeny and Dr. Rajesh Menon for their unmitigated support.

C H A P T E R 1

INTRODUCTION

Surface enhanced Raman spectroscopy (SERS) is a powerful analytical tool used to identify chemicals at very low concentrations 0.1-100 ppb [1, 2]. Whenever incident electromagnetic radiation interacts with the electron cloud of molecules, it results in numerous scattering events. These scattering events can be either elastic or inelastic. Figure 1 shows the important working principles of micro-Raman spectroscopy and SERS. In general, inelastic scattering comprises about 0.001% of all scattering events.

Elastic scattering is where the emitted photon is of the same energy as the incident photon and is known as Rayleigh scattering, while inelastic is where the emitted photon is of either lower or higher energy compared to the incident photon and is known Stokes and Anti-

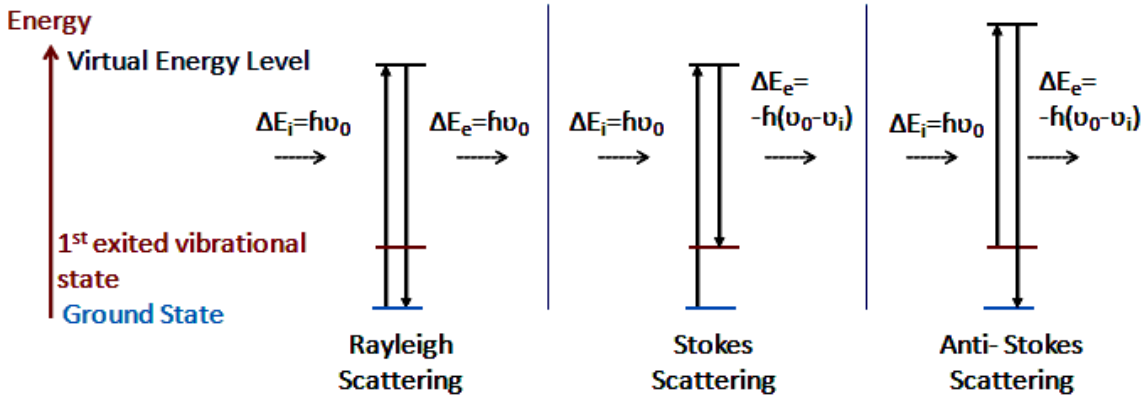

Figure 1: *Diagram portraying elastic and inelastic scattering events in energy band diagram. Inelastic scattering (Stokes and Anti-Stokes) events contribute to Raman scattering.*

Stokes scattering, respectively. It is these inelastic scattering events that contribute to Raman signals.

It is noted that molecules adsorbed near or at the surface of certain nanostructures result in strongly increased Raman signals [2]. Such phenomena is attributed to the concentration of electromagnetic (EM) optical fields at "hotspots" that usually occur at nanoscale junctions or clefts in metal nanostructures [2]. Electrochemically roughened gold electrodes [3], silver colloidal nanoparticles deposited on roughened silver surfaces or AgO films deposited on glass slides [3] and microfabricated nanostructures coated with SERS active material (such as silver and/or gold) [3] are but a few examples of substrates reported so far. A new technique is the use of dielectrophoresis (DEP) force to induce local aggregation [4] of particles (such as silver or gold nanoparticles). An attractive aspect of DEP is that it can be used while monitoring SERS to track and halt or modify the Raman spectra in real time by changing the DEP conditions such as voltage (or current), frequency and DC bias. Figure 2 shows the important working principles of DEP.

Strictly speaking, DEP is the motion of an uncharged (neutral) particle caused by the polarization effect in a nonuniform electric field [5]. It can be concluded that gold nanoparticles (NP) coated with a self assembled monolayer (SAM) to prevent coagulation of the particles are slightly positively charged. In this case, the DEP force depends on the Nanoparticle (NP) charge, possible induced dipole and the electric field gradient [5]. DEP has been developed extensively for manipulating particles in biology to separate, trap, sort and translate cells, viruses, proteins and DNA [6].

DEP, when combined with DLA, results in the formation of nano- and microstructures capable of enhancing Raman signals by incorporating the unknown molecules in the fabric of these wires and exposing them to electromagnetic fields in the crevices and openings of the nanowires (NW) with dense fractal geometries.

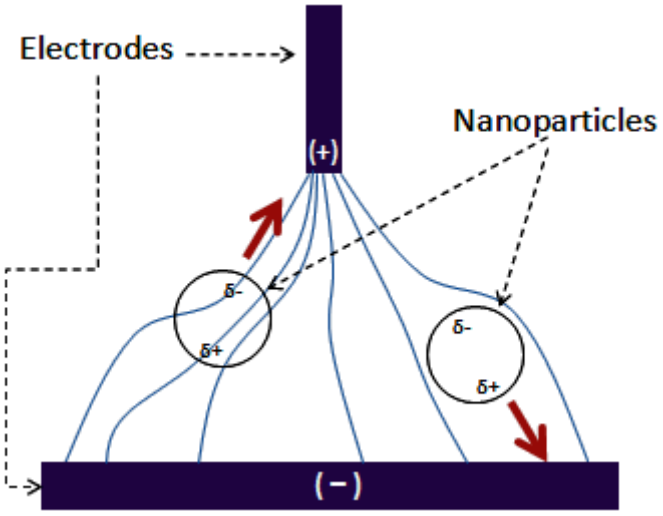

Figure 2: *Nonuniform electric field setup using asymmetric electrodes results in polarization within neutral nanoparticles and hence causes Dielectrophoresis.*

Diffusion Limited Aggregation is a process where Brownian motion causes particles to experience a 'random walk' and cluster together to form aggregates [7] (see Figure 3 and Figure 4). Such a phenomenon is applicable to any system where diffusion is the principal means of transport. Such clusters are known as Brownian Trees and are examples of fractals.

This thesis investigates the ability of DEP to form NWs that uniformly incorporate the unknown molecules in a dense array of randomly distributed NPs. These NPs nearly touch each other to form an electromagnetic vise around unknown molecules, subjecting them to large fields and returning their interaction information to the optical detector, as schematically shown in Figure 3.

The high dielectric constant, which occurs in heterogeneous media, and the dielectric dispersion that occurs in a wide range of frequencies, suggests that both volume and surface properties are important in its study [8]. Numerous physical processes have been attributed to the

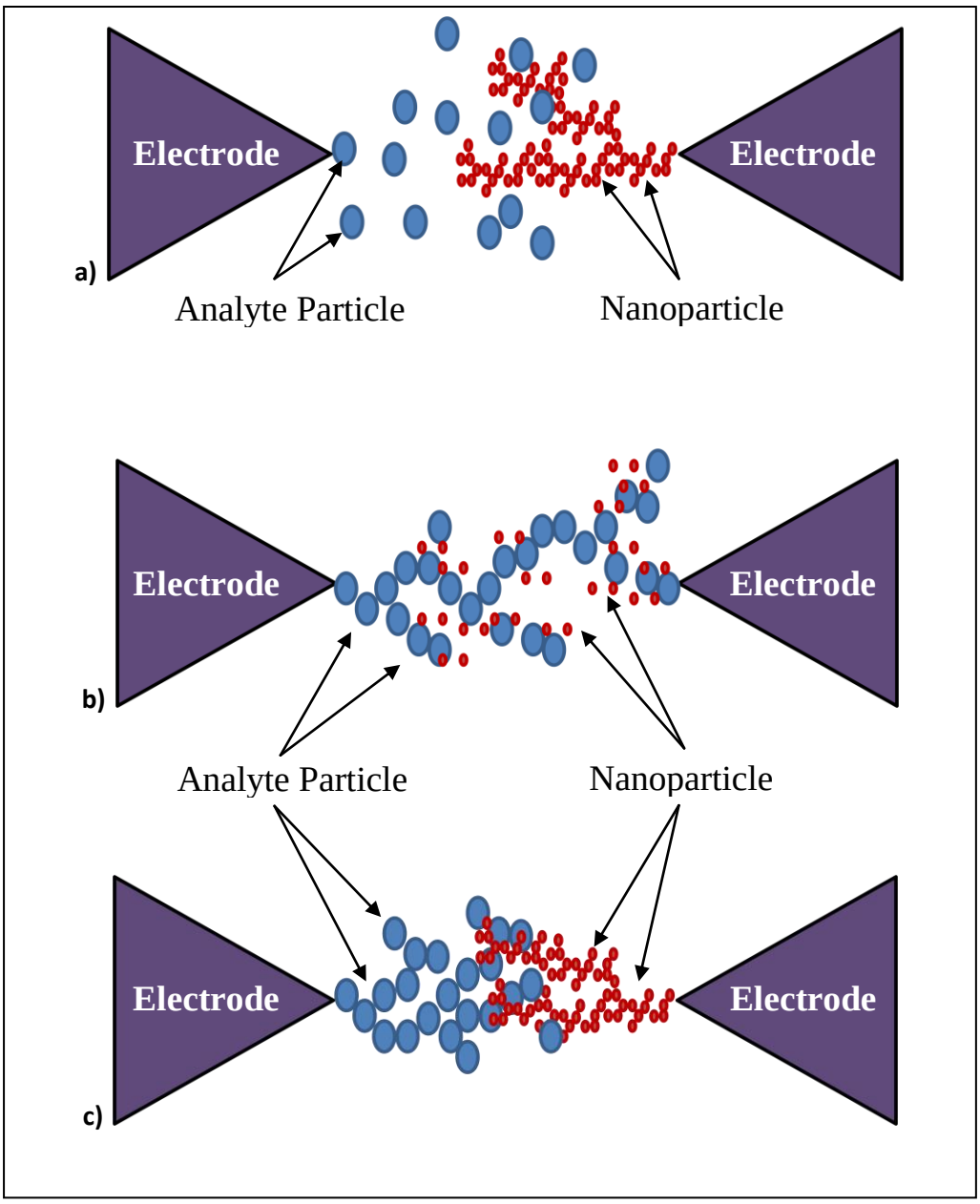

Figure 3: *Schematic of DEP nanowires incorporating the unknown molecules for enhanced Raman spectroscopy at: a) frequency corresponding to τ_1. b) DEP conditions changed so that frequency now corresponds to τ_2 ($\tau_2 < \tau_1$). c) If DEP conditions are changed so that frequency now corresponds to τ_3: $\tau_2 < \tau_3 < \tau_1$, the DEP can cause separation.*

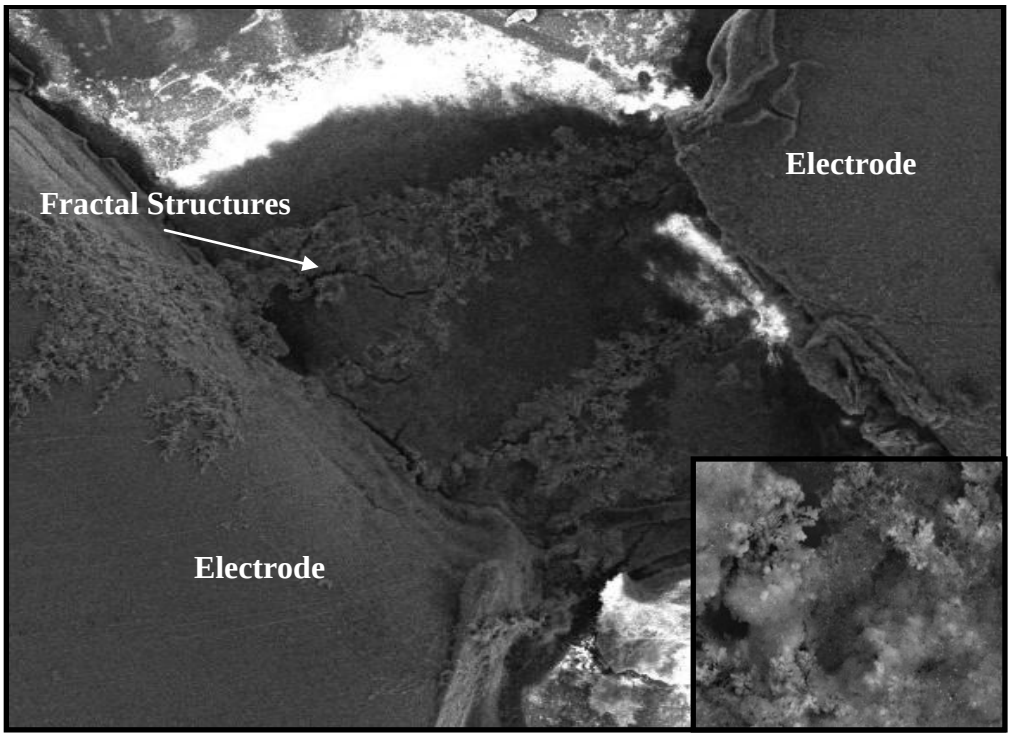

Figure 4: *SEM images of DLA structures formed due to DEP. (Inset: image shows the fractal geometric structures that lead to high SERS enhancement).*

enhanced polarizability of disperse systems such as Interfacial (Maxwell-Wagner) polarization, Electrophoretic dielectric response, Surface-modified interfacial polarization, etc. [8]. In all the systems mentioned, the principal physical parameters are the characteristic relaxation time of the process, τ, and the magnitude of the dielectric increment, ΔK. 'τ' provides a measure of the frequency range for which the particular mechanism is effective, while, ΔK gives a measure of the intensity of the particular mechanism.

Using the Interfacial (Maxwell-Wagner) model, it can be deduced that in suspensions of particles in liquids, an effective dipole appears to form when charges accumulate at the particle-solution interface. When particles are induced to move towards the electrodes, it is assigned the term Positive DEP, while when the particles are induced to move away from the electrodes, it is

known as Negative DEP. Also, at very low frequencies, the polarization readily follows the changing field (and the contribution to the dielectric constant is maximum), while on the other hand, at high frequencies, the field alternates too quickly for the interfacial polarization to arise (and little contribution to dielectric constant). At an intermediate frequency, the polarization lags behind the field and energy is more strongly dissipated. In the simple case of two media, a maximum characteristic frequency, f_m, can be defined, which is related to the characteristic relaxation time, τ [8].

$$\tau = 1/(2\pi f_m) = 1/\omega_m \qquad (1)$$

As a result, it can be stated that due to the disparity in permittivity of the gold nanoparticles and the thymine particles in our sample solution, the formation of the fractal structures are selective with respect to frequency. It may well be the case that at one particular frequency (corresponding to τ_1), the gold nanoparticles begin to form DLA structures, while thymine remains scattered, while at another (predictably lower) frequency (corresponding to τ_2), thymine particles may begin to form DLA structures, and the gold nanoparticles remain scattered. Such a situation, although not encountered during our experimentation, deems the possibility that a compromise (or intermediate) frequency (corresponding to τ_3: $\tau_2<\tau_3<\tau_1$) exists where both gold nanoparticles and the thymine would form DLA structures simultaneously. Figure 3 illustrates the probable effects schematically.

C H A P T E R 2

EXPERIMENTAL DESIGN

A schematic of the experimental setup for the Raman interrogation is illustrated in Figure 5. It consists of a quartz slide onto which Copper electrodes are placed using Copper tape in the form of triangles where the apexes are spaced apart by several hundred microns. This ensures the generation of nonuniform E-field at the tips between each electrode. The copper electrodes are connected to an oscilloscope and a frequency generator, allowing control and monitoring of applied voltages. The analyte mixture is placed in the center, between the electrodes and once a voltage is applied, the Raman laser is used for interrogation.

2.1 Quartz Substrate

Quartz slides were used because of their distinct Raman peak at 463cm^{-1} and lack of influence in other bands. These Quartz slides were cut away from Quartz discs (purchased from Crystal Technology) using a diamond scribe. The slides were then thoroughly cleaned several times with Acetone and distilled water to ensure no organic matter remained that could potentially influence the Raman spectrum. The Quartz slides had a single surface polished while the opposite side was roughened. Both surfaces, however, depicted the same Raman peak corresponding to Quartz (463cm^{-1}).

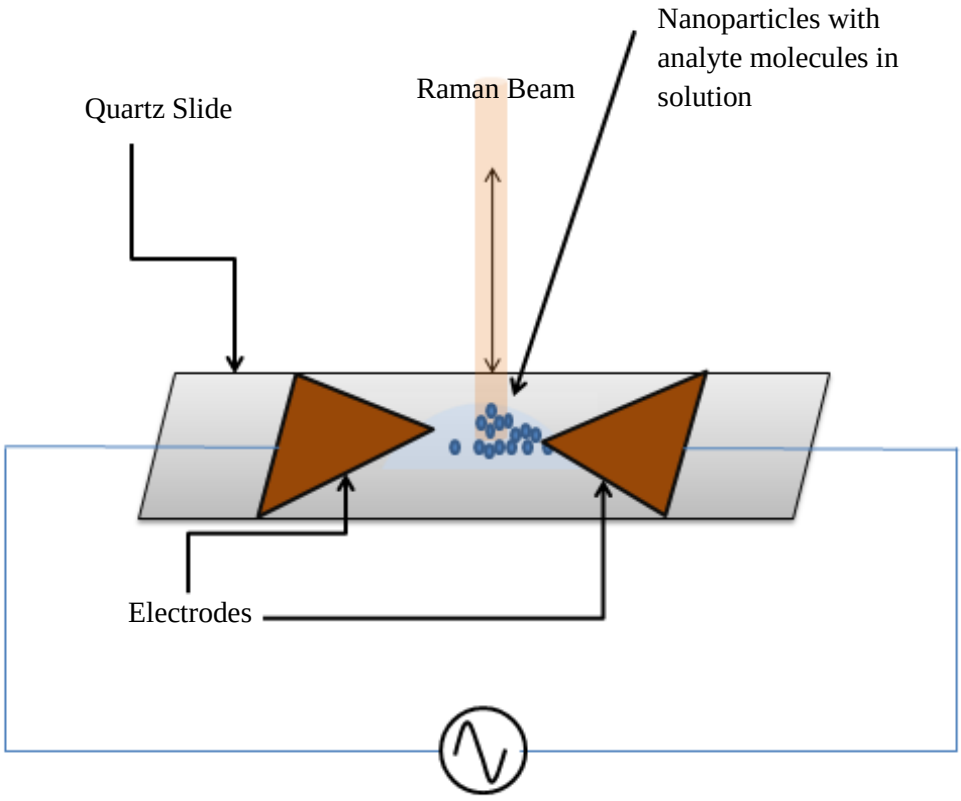

Figure 5: *Schematic diagram of SERS experimental setup.*

Copper tape was then glued on to the Quartz slide using commercially available "ACE All-Purpose Super Glue" and two diagonals were cut away and removed using an "X-acto" knife. The resulting triangular structures that remained glued to the Quartz had spacing on the order of 100s of microns. These structures were used as the electrodes for dielectrophoresis, as shown in Figure 5 and Figure 6. The slide was once again thoroughly cleaned using acetone to ensure no glue residue remained.

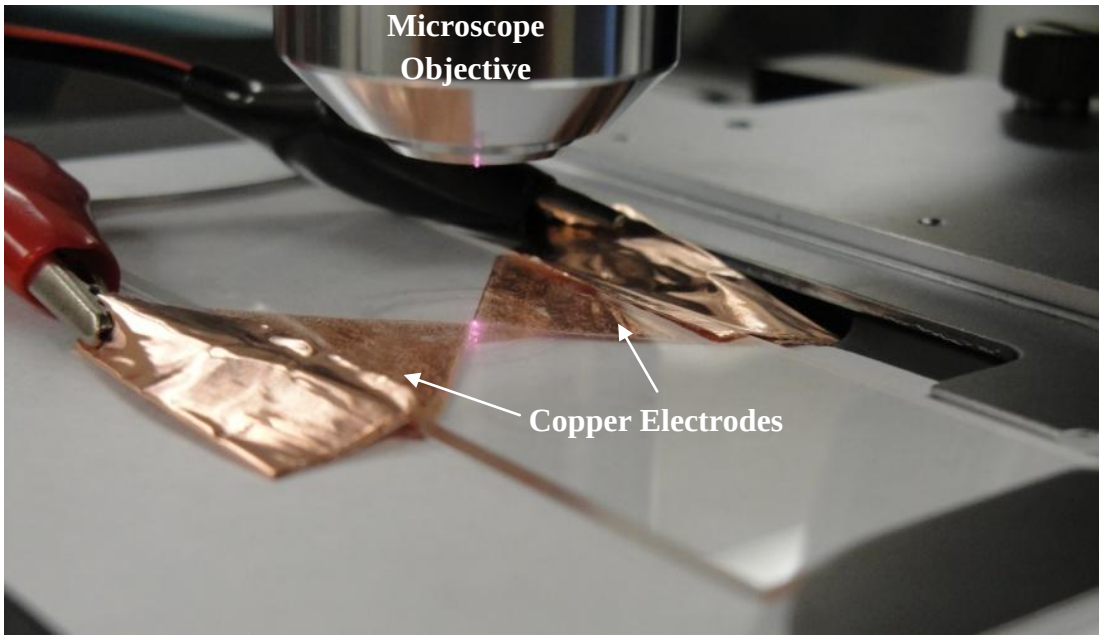

Figure 6: *Slide with sample being interrogated by Raman laser.*

2.2 Preparation of Solutions

Colloidal gold solution, purchased from BB International, was used as purchased. The nanoparticles, which were sized at an average of 101.5nm and had a concentration of 9.299×10^{-12} mol/dm^3, were ultrasonicated for 12 minutes prior to use. NaCl solution of concentration 0.02M was prepared using NaCl purchased from Sigma. A solution of thymine, having concentration 19.03µM, was carefully prepared using Thymine 99% purchased from Sigma.

5ml of the 19.03µM thymine solution was mixed with 5ml of gold colloidal solution and ultrasonicated for 8 minutes. Another solution consisting of 5ml 19.03µM thymine solution, 5ml gold colloidal solution and 2ml of 0.02M NaCl solution was also prepared and ultrasonicated for 8 minutes.

Essentially, two samples were prepared – one containing gold nanoparticles with NaCl solution and Thymine, while the other included Thymine, but excluded NaCl solution.

2.3 Diffusion Limited Aggregation Induced Fractal Geometric Structures

Figure 7 shows the formation of fractal geometric structures induced by Diffusion Limited Aggregation within the sample solution mixture. This was used as the substrate for SERS.

A single drop of the first sample (gold colloidal solution with Thymine) was carefully placed in between the electrodes and its "growth" was observed through a microscope (Olympus BX51). Using a setup that was comprised of an AC source (GW Instek GFG-8020H) and Oscilloscope (Tektronix 2230 Digital Storage Oscilloscope), the electrodes were connected and the power turned on. Through delicate and meticulous control of the applied DC bias and applied AC voltage, the structures were successfully grown on all instances that the experiment was conducted. A DC bias of approximately 1V and an AC voltage of about $12V_{p-p}$ with a frequency of around 1.8Khz (or 10.8Khz) was just right to begin the generation of fractal structures (Figure 5). The same procedure was also used on the sample that included NaCl solution.

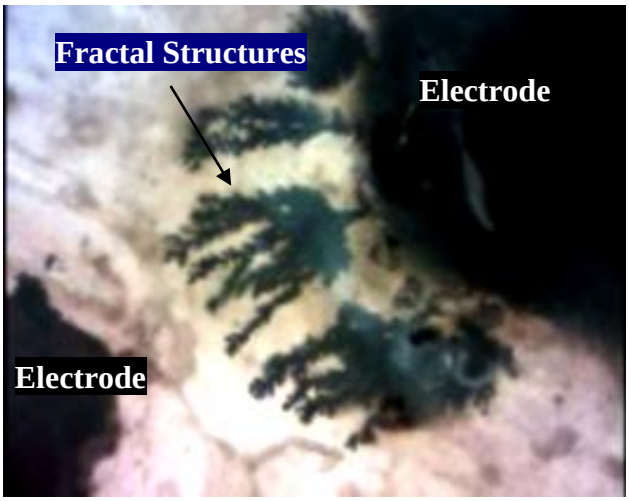

Figure 7: *Image showing the growth of fractal geometric structures formed by Diffusion Limited Aggregation of gold nanoparticles induced by Dielectrophoresis.*

2.4 SERS Measurements

The micro-Raman system used to obtain Raman spectra comprised of a Deltanu ExamineR 785 module coupled to an Olympus BX51 microscope, as shown in Figure 8. A 10X objective primarily was used to transmit and collect incident and scattered light. The module comprised of a diode laser (785nm wavelength) at 120mW (adjustable) and resolution of the obtained Raman spectrum was 5 cm^{-1}. The time of integration was fixed at 10s.

Several spectra were taken at varying solution parameters in order to determine the effectiveness of the fractal geometric structures. In addition, the spectrums were always obtained taking a reference spectrum before the actual spectrum. This further ensured accuracy of the samples' Raman spectrum. The most important spectra that were obtained are compared and discussed in the following section.

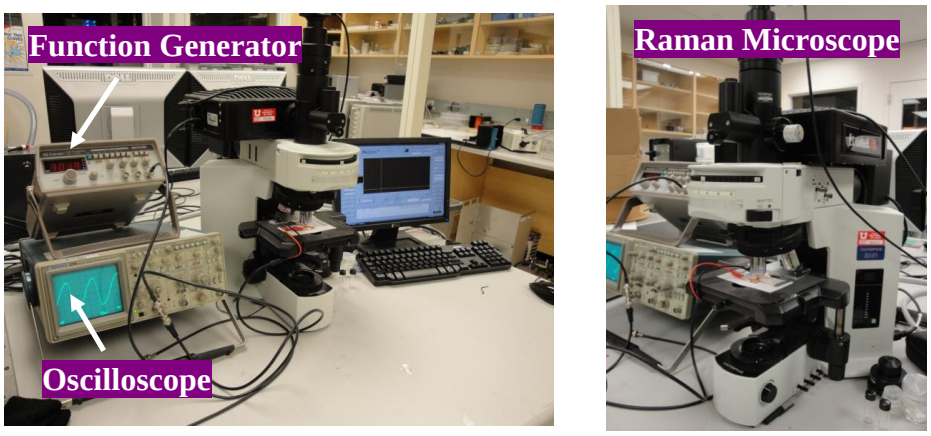

Figure 8: *Raman spectrometer setup (comprises oscilloscope, function generator and Raman microscope).*

CHAPTER 3

RESULTS

Using the fractal geometric structures, incredibly large SERS enhancement factors up to 10^9 were obtained. The Raman spectra that were obtained for analysis are shown and explained in this chapter (Figure 9 to Figure 13). Each spectrum was obtained using the spectrometer, as explained in the previous section, the data were captured using the Raman Microscope objective, and saved into a Microsoft Excel file, using the DeltaNu software. The graphs were next plotted and presented as given here. The spectra that are discussed range from Raman signatures obtained from the following conditions, respectively: quartz slide alone; solid Thymine sample; mixture of gold colloids, NaCl solution, Thymine solution and in the absence of fractal geometric structures; mixture of gold colloids, Thymine solution, presence of fractal geometric structures and the absence of NaCl solution; and finally, mixture of gold colloids, NaCl solution, Thymine solution and in the presence of fractal geometric structures. Each spectrum is presented as was obtained within the Wavenumber range of 200cm^{-1} to 2000cm^{-1} and an arbitrary intensity peak (determined by the CCD and DeltaNu software).

Upon examination of the resulting spectra, it is clearly seen that presence of fractal geometric structures dramatically amplify the peaks present due to Thymine within the solution mixture. Sample mixtures without fractal geometric structures present no visible amplification to Thymine Raman spectra peaks.

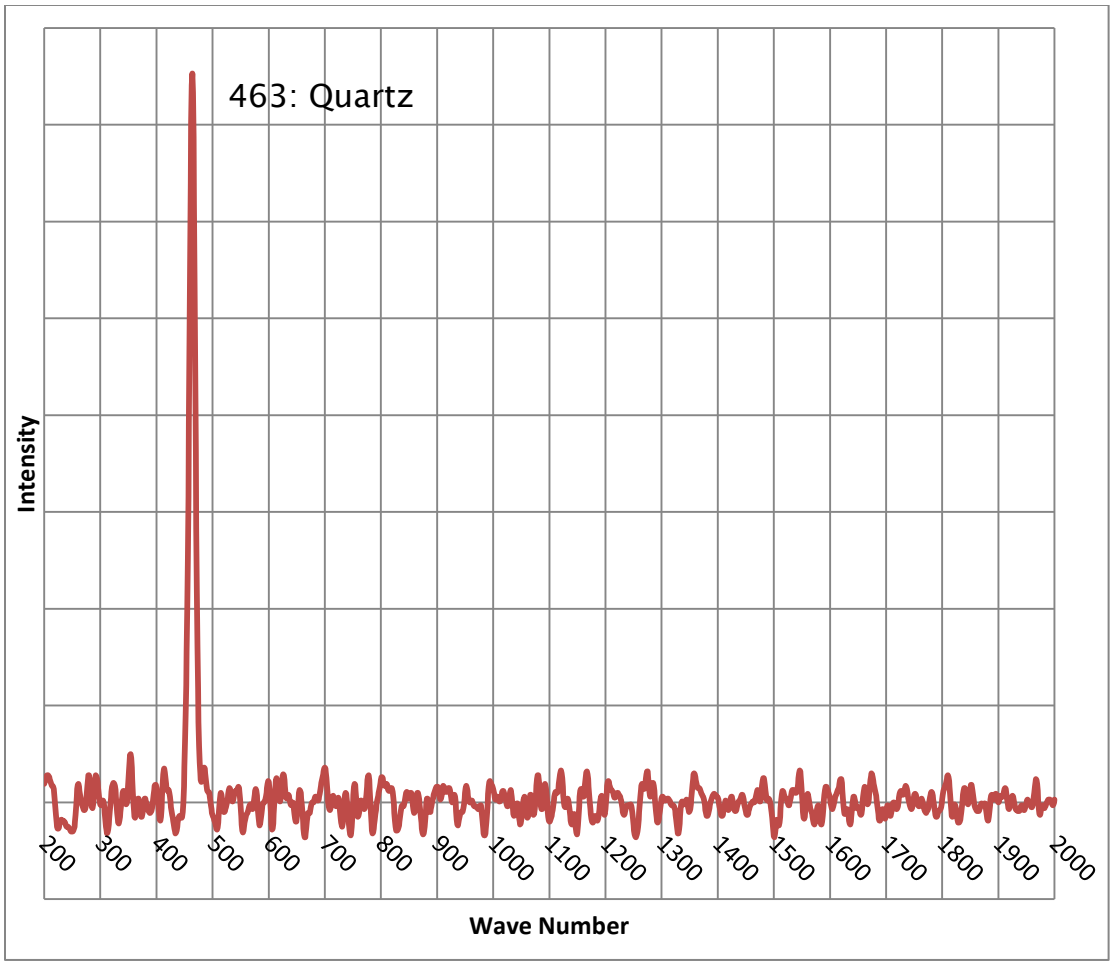

Figure 9: *Raman spectrum of Quartz slide alone.*

The spectrum in Figure 9 was taken over Quartz substrate and considered to be a control in order to compare and eliminate any background signatures that may contribute to the actual SERS spectrum to be obtained on the fractal geometric structures. It can be seen that a prominent peak at 463cm^{-1} corresponding to Quartz is visible. The rest of the spectrum appears relatively flat, indicating the absence of any other materials that exhibit any Raman signature. Based on the fact that only a single prominent peak shows up during Raman interrogation, Quartz was selected as the substrate for the experiment.

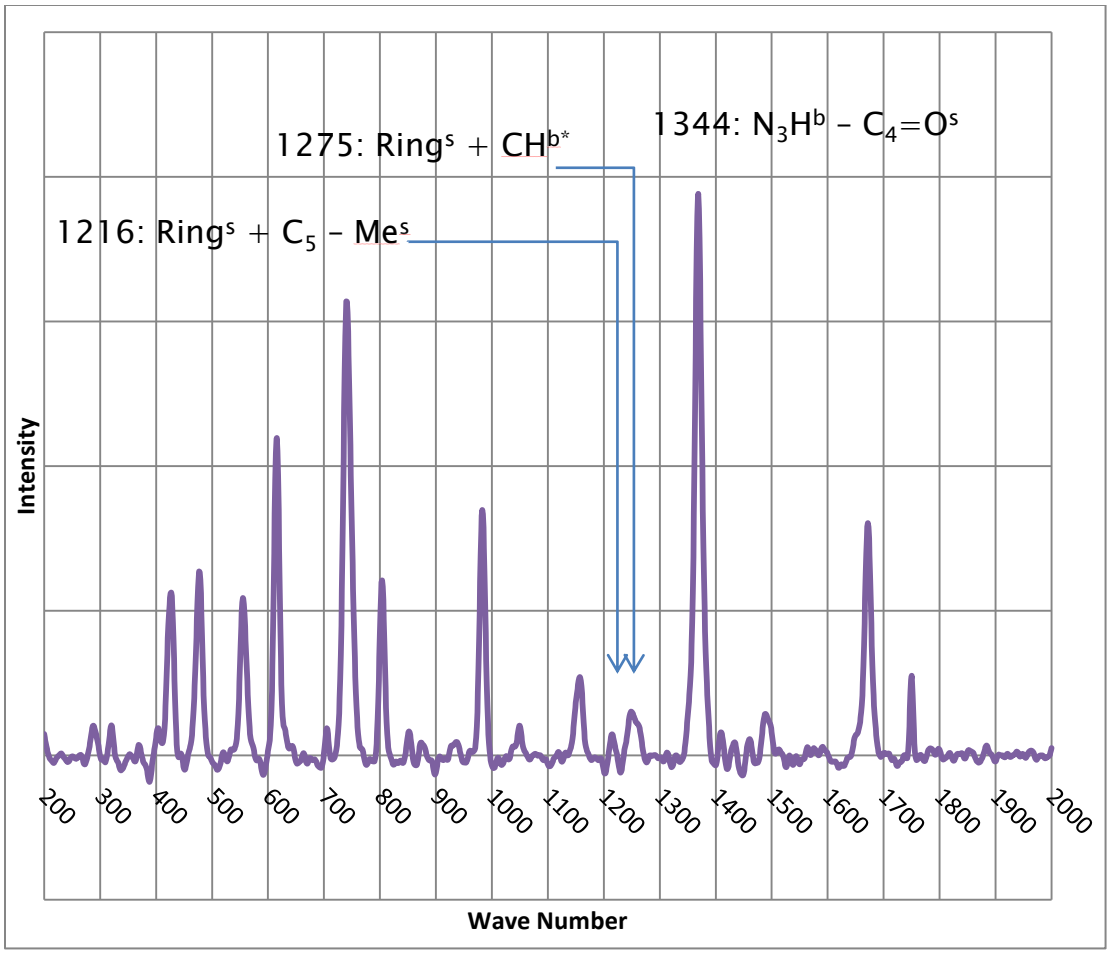

Figure 10: *Raman spectrum of solid Thymine sample.*

The spectrum shown in Figure 10 was also a control spectrum taken over a sample of solid Thymine powder. This spectrum allowed us to attribute peaks that directly correspond to those formed due to presence of Thymine. The various peaks and the characteristic bonds that they correspond to are indicated in the spectrum of Figure 10. It was these distinct peaks that were indicative of the presence of micromolar concentrations of Thymine in the spectra that were obtained after the novel SERS substrate was grown.

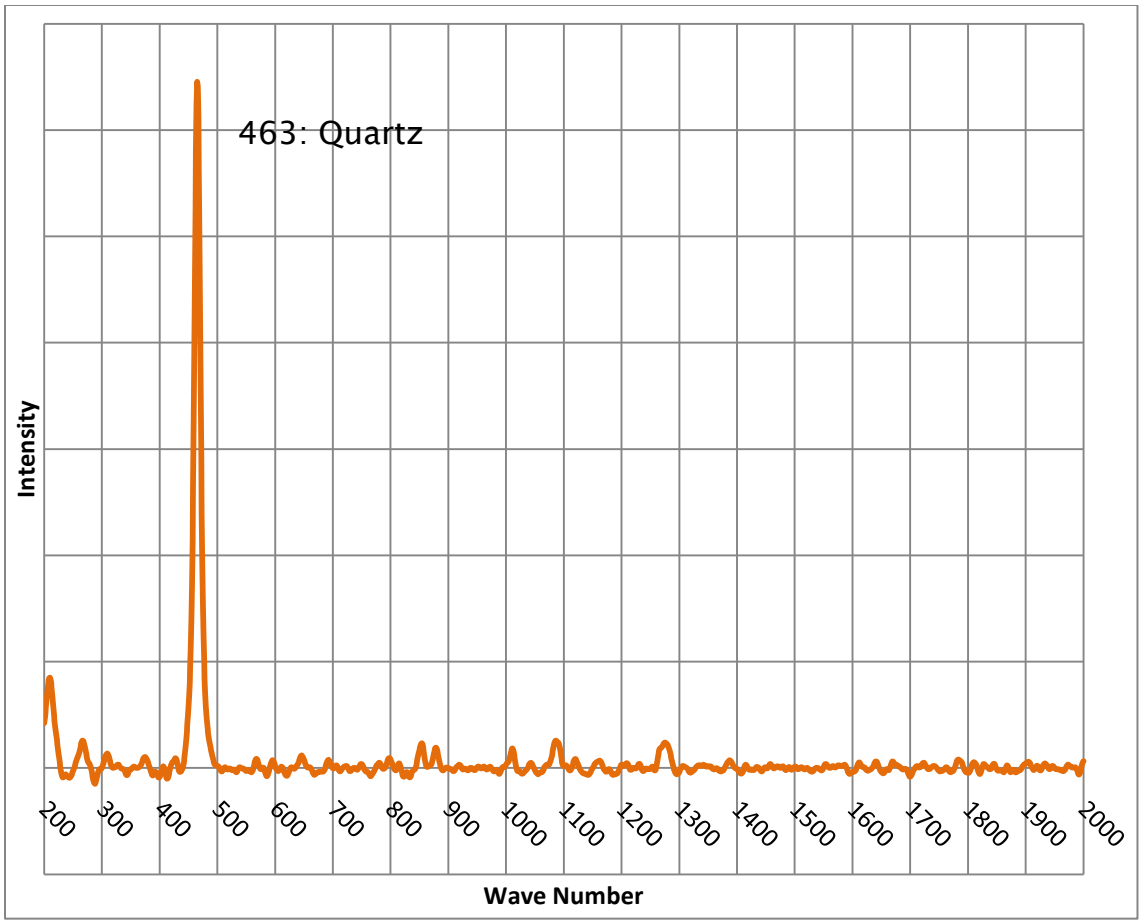

Figure 11: *Raman spectrum of gold colloids + NaCl solution + Thymine solution. No fractal structures present.*

A third control spectrum is shown in Figure 11. This was taken from the sample solution containing gold colloids, NaCl solution and thymine in solution. Note that this spectrum was obtained prior to the formation of SERS active fractal geometric structures. This spectrum shows that before the formation of fractal geometric structures, the solution mixture, itself, did not portray any significant peaks corresponding to Thymine. However, one distinct peak due to Quartz, at 463cm^{-1}, is visible.

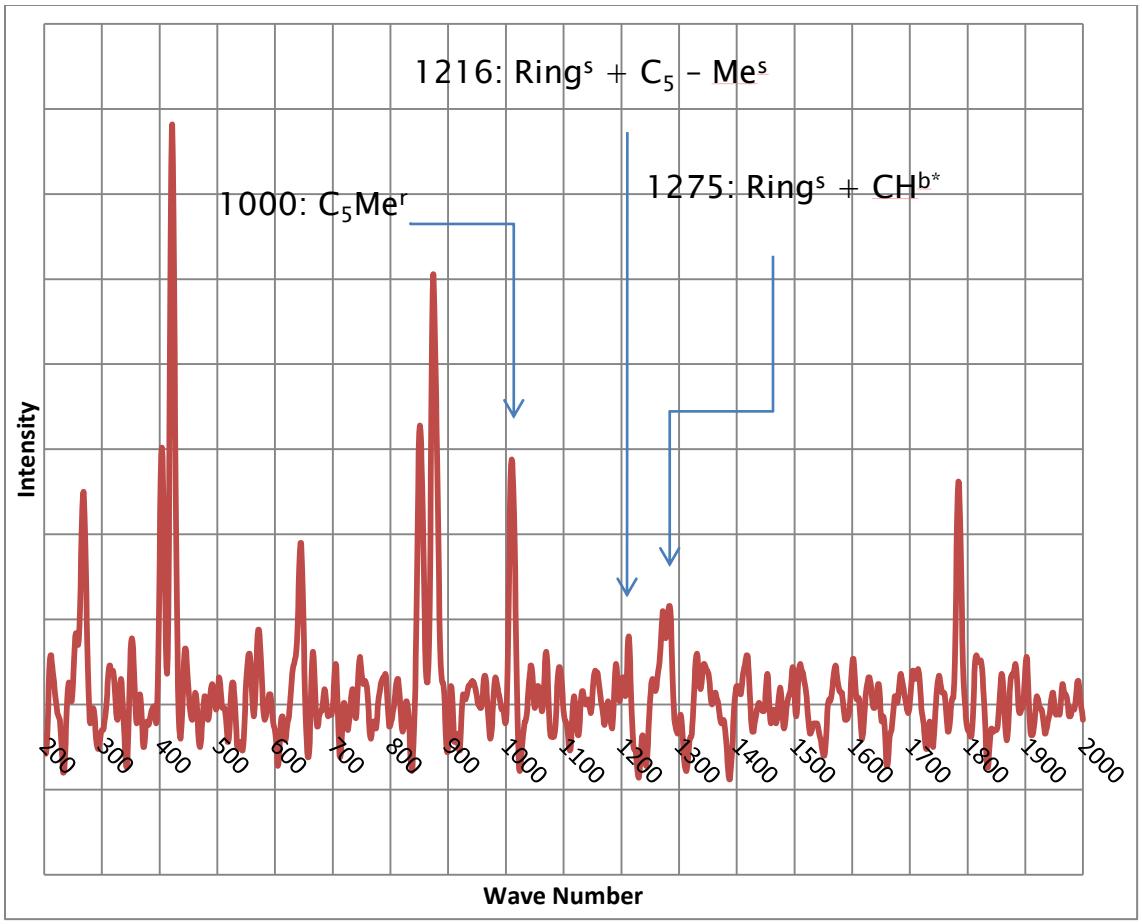

Figure 12: *Raman spectrum of gold colloids + Thymine solution + fractal geometric structures. (No NaCl solution present).*

Figure 12 compares the Raman spectrum obtained from Thymine, after being treated with gold colloids and NaCl solution on the formation of fractal geometric structures. It is readily observed that an enhancement is observable for the micromolar concentration of Thymine. On one hand, it is seen that Thymine mixed in gold nanoparticles (Figure 9) generates hardly any Raman signal enhancement, while, on the other hand, with the formation of fractal geometric structures, an enhancement is readily visible in the 430, 800, 1000 and 1200-1300 cm^{-1} peaks (Figure 11). It can also be seen that the addition of NaCl solution to the colloidal solution of gold

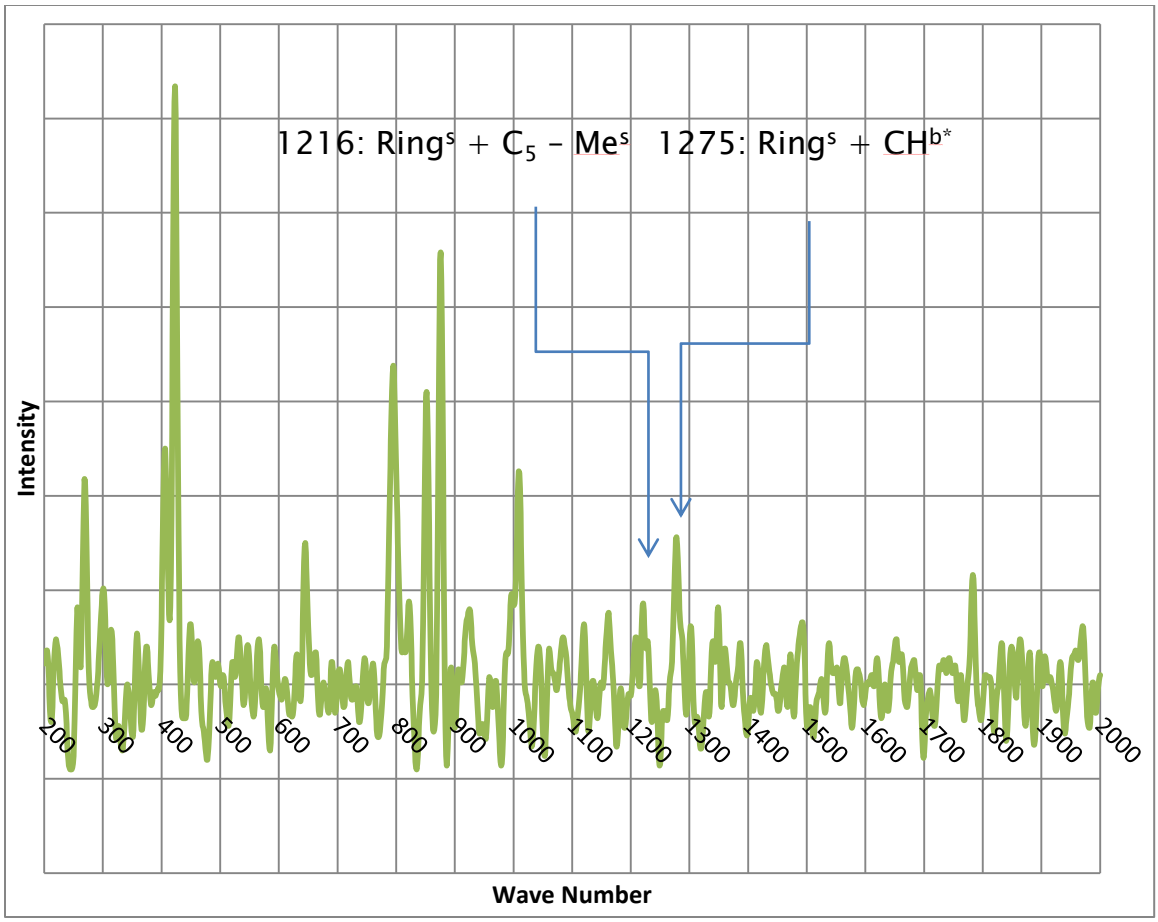

Figure 13: *Raman spectrum of gold colloids + NaCl solution + Thymine solution + fractal geometric structures.*

nanoparticles, Thymine, and with the formation of fractal geometric structures, causes similar, if not somewhat greater, enhancement (Figure 12 and Figure 13) in those respective bands.

Figure 14 (along with Table 1) provides a summary of all the Raman spectra that were obtained and used to compare and evaluate the effect of fractal geometric structures on the Raman signature of micromolar concentrations of Thymine in solution. By superimposing all the obtained spectra, it is evident that the nanowire formations enabled a dramatic response for Thymine peaks.

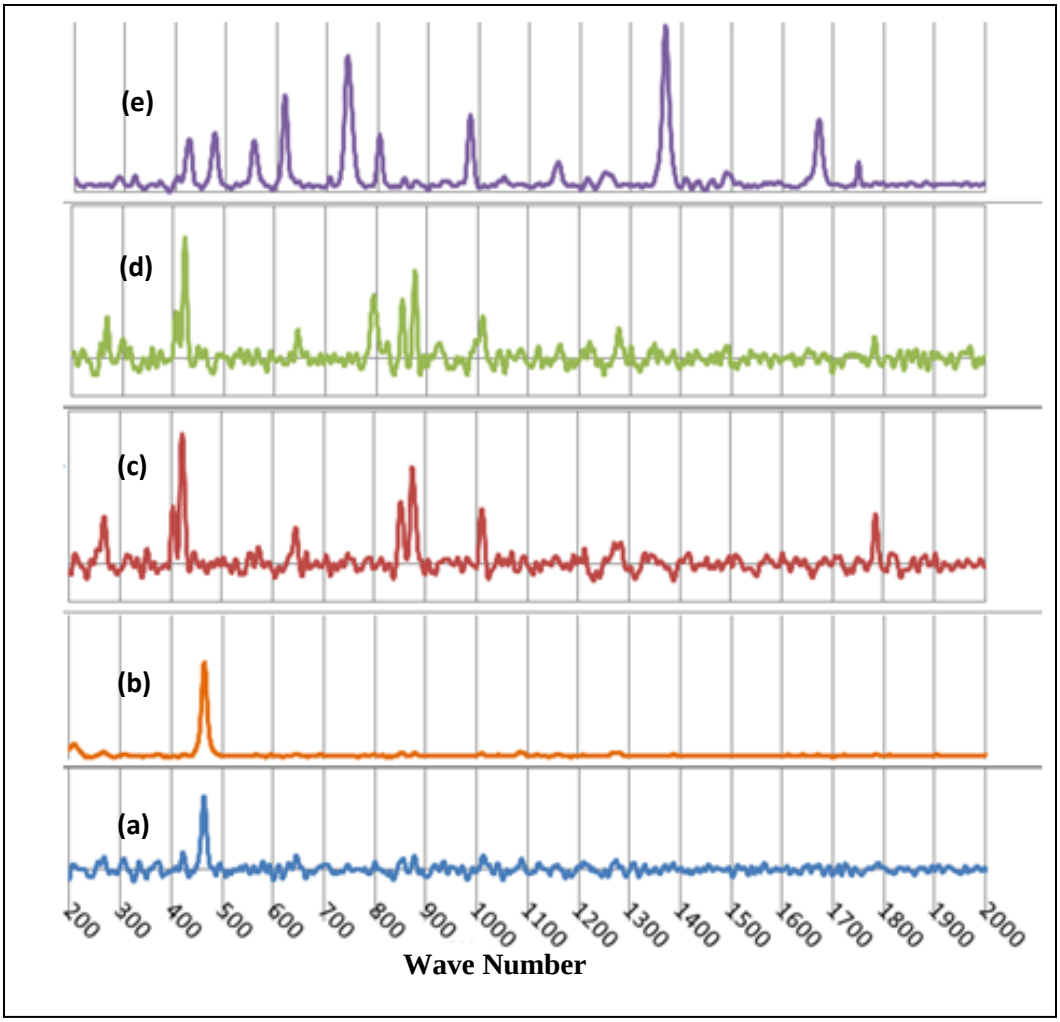

Figure 14: *Spectra compared from different experimental conditions: (a, b, c and d contain gold colloids) (details in Table 1).*

Table 1: *Summary of analytes that were Raman interrogated shown in Figure 14.*

Spectrum	*Gold Colloids*	*NaCl Solution*	*Thymine*	*FG Structures by DEP*
(a)	*Yes*	*No*	*Yes*	*No*
(b)	*Yes*	*Yes*	*Yes*	*No*
(c)	*Yes*	*No*	*Yes*	*Yes*
(d)	*Yes*	*Yes*	*Yes*	*Yes*
(e)	*Raman Spectrum of Solid Thymine on Quartz Substrate*			

The enhancements calculated for Thymine in DEP induced DLA of the gold nanoparticles (excluding NaCl solution) resulted in an enhancement factor of $\sim 5.75 \times 10^6$, while that for the case including NaCl solution resulted in an enhancement factor of $\sim 5.54 \times 10^6$, which is of similar order. From taking into account the number of gold colloids per ml (according to datasheet), and the number of Thymine molecules in the resulting laser interrogation volume, where we assume approximately 4 active sites per nanoparticle, we end up with roughly 500 active sites within the laser interrogation volume. This is 10^6 times smaller, resulting in an enhancement factor ~10^9. From Figure 11, it is evident that NaCl solution on its own provides no enhancement.

CHAPTER 4

ANALYSIS / DISCUSSION

4.1 SERS Enhancements and Explanations

The large enhancements in our experimental evidence can be strongly attributed to the long range optical EM fields at the "hotspots" near interstices or nanoscale junctions around the gold fractal geometric structures. The intricate NW structures induce local surface plasmons on the aggregated gold structure and enhance the Raman scattering near its nanometric volume [14].

The SERS intensity is most efficient when the sample's molecule has a polarizability component perpendicular to the surface [1]. As is the case with Thymine, the plane of the ring will provide the highest polarizability. Also, it is known that the orientation of the molecules with respect to the substrate plays an essential role in providing an efficient Raman scattering [1]. As a result, the high enhancement of the Thymine Raman signal can be attributed to the fact that, as the NWs are not all completely parallel to the quartz substrate, some do vary in their angular orientation. As a result, some of these fractal formations may be perpendicular to the Thymine molecules and thereby provide a very efficient Raman scattering.

Further enhancement, evident from Figure 13, is due to the addition of NaCl solution. This effect requires further investigation for a decisive explanation to the cause; however, it may be attributed to the Cl^- ions of NaCl solution [10]. One explanation could be that the anion gives a large enhancement for the fractal structure because it being monovalent provides greater electrostatic interactions for Thymine and the fractal structure than if it were absent.

4.2 Peaks Corresponding to Thymine

The peaks corresponding to Thymine (on a quartz substrate) are shown in Figure 10 in the previous section. The structure of a Thymine molecule is shown in Figure 15. It is known to have its Ring Breathing mode at 750cm^{-1} and it is very clearly evident from Figure 14(c) and Figure 14(d) how that peak is clearly enhanced, although shifted to 800cm^{-1}, with the fractal geometric structure providing a significant part of the EM enhancement.

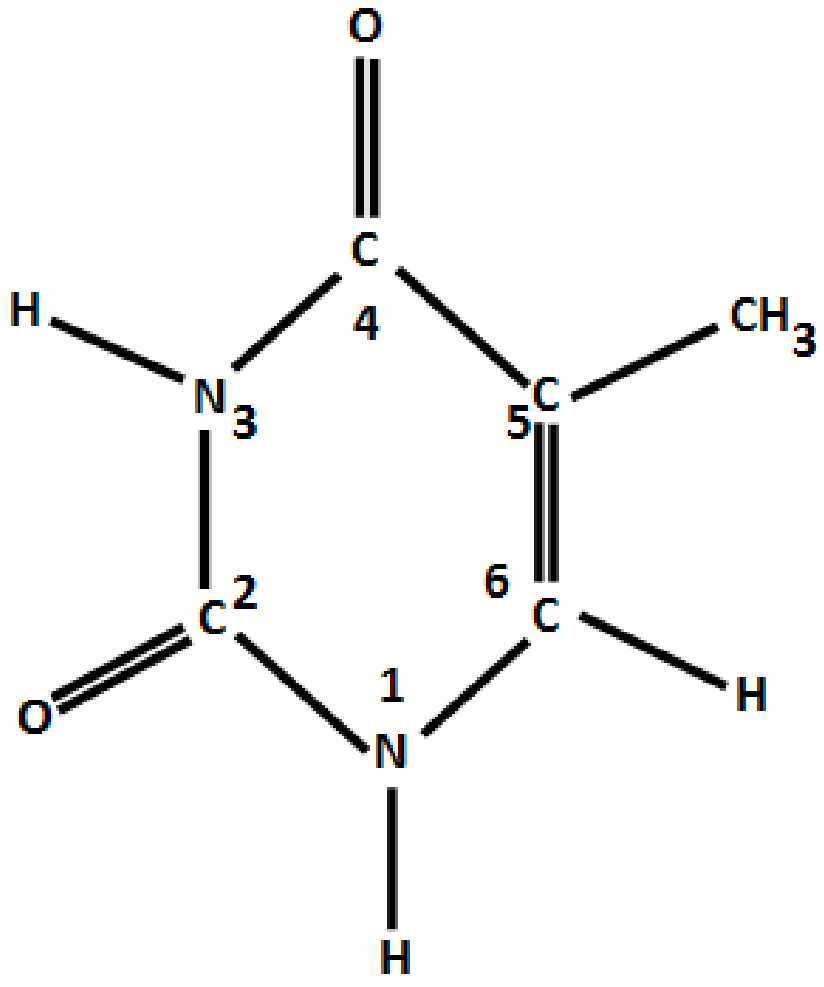

Figure 15: *Structure of Thymine.*

Peaks at 1000, 1216, 1275 and 1344 cm-1 are caused by the following structures (refer to Figure 8) (superscripts: r=rocking, s= Stretching, b=bending):

1000: C_5Me^r

1216: $Ring^s + C_5 – Me^s$

1275: $Ring^s + CH^{b*}$

1344: $N_3H^b – C_4=O^s$

(*Source: Ref. 8*)

From Figure 14(c) and 14(d), it can be confirmed that the peaks correspond to those distinctive to Thymine.

4.3 Enhancement Factor

The SERS Substrate Enhancement Factor (SSEF) was calculated using the following equation [2, 12]:

$$SSEF = \frac{I_{SERS}}{I_{Powder}} \times \frac{N_{Powder}}{N_{SERS}} \qquad (2)$$

where,

I_{SERS} = SERS intensity due to Thymine in solution,

I_{powder} = Intensity due to thymine in powder form

N_{powder} = Number of molecules of Thymine in powder form that contributed to creating I_{powder},

N_{SERS} = Number of molecules of Thymine in solution that contributed to creating I_{SERS}

Bearing in mind that the laser spot size was approximately 23μm in diameter, and assuming that the excitation volume was the form of a cylinder, the number of particles in the Thymine powder that contributed to the Raman signal was estimated at 4.2×10^{15}. This assumption underestimates N_{powder} since, in reality, the excitation volume is in the form of two back-to-back truncated cones whose waist diameter is that of the laser spot [2].

The concentration and volume of Thymine in the sample solutions (7.93×10^{-6}M and 0.05ml (about 1 drop), respectively) containing gold colloids and NaCl solution and the use of DEP induced DLA placed on the slide for Raman analysis yields approximately 6.33×10^{7} particles contributing to the Raman scattering under laser interrogation. The number of particles for the sample containing Thymine in gold colloids *without* NaCl solution yielded around 7.59×10^{7} Thymine particles contributing to Raman scattering under the laser interrogation. The number of particles was of the same order, yet the sample which included NaCl solution delineated a weakly higher enhancement.

The enhancement factor, essentially, bearing in mind the assumption of approximately 500 active nanoparticles sites, resulted in ~10^{9}.

4.4 Further Work

Other substrates have been prepared and were experimented upon during the course of this investigation. Some novel ideas included using single thin fiber optic strands forming interleaved interdigitated structures. These structures afforded great optimism as effective SERS substrates when a thin layer of silver was sputtered upon them. More importantly, the effect of a perpendicularly applied electric field on the analyte was examined by varying the applied frequency and obtaining Raman spectra, respectively. Although more work is required in this area before any strong conclusions can be drawn, it can be stated that, on preliminary observation, a response was obtained for electric field variations. The structure that was tested is shown in Figure 16 and Figure 17.

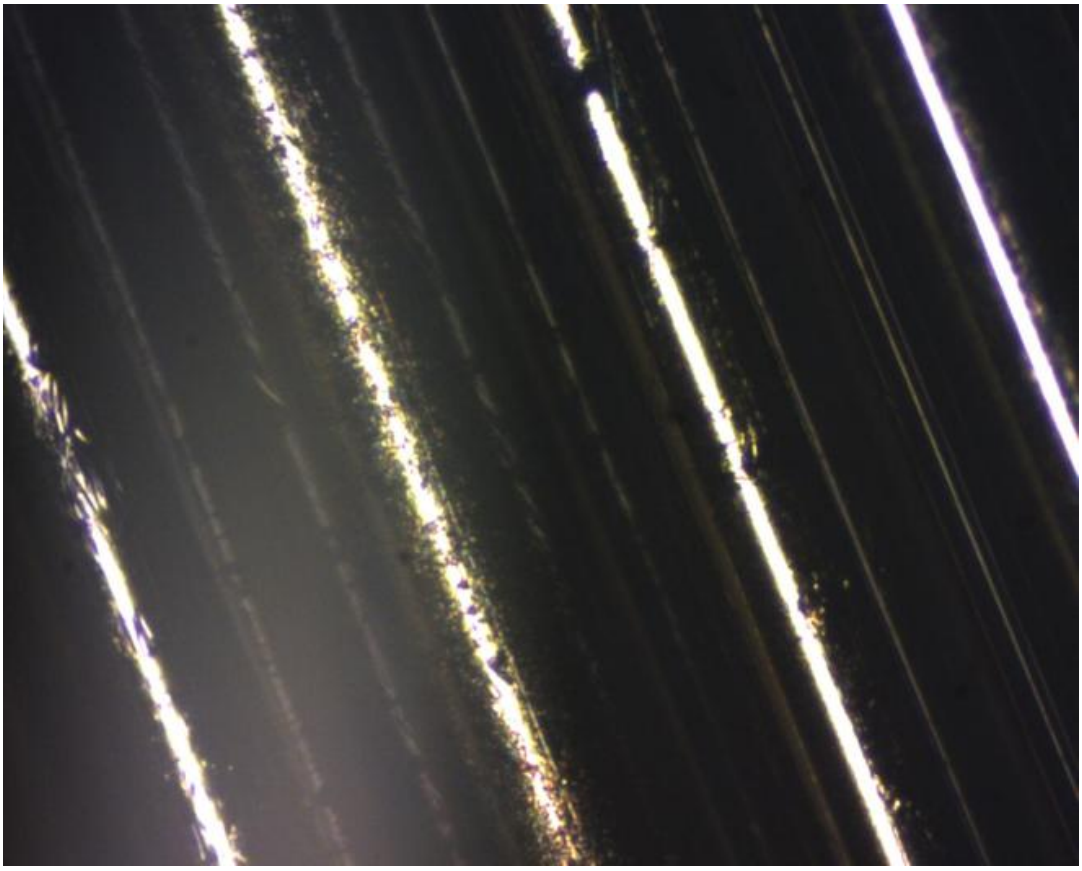

Figure 16: *Image of interdigitated fiber optic strands with thin silver coating.*

The image on Figure 16 is a picture of where the Raman laser was focused on a section of the silver-coated substrate as seen in Figure 17. The concept behind the investigation was based on the fact that at the junction between two cylindrical optical fibers, a silver-coated nanoscale gap may result in high SERS enhancements. Also, using this setup, the effect of introducing E-fields between each fiber optic cable can also be investigated. With application of E-fields on silver-coated interdigitated fiber-optic "fingers," any variations in SERS may be observed.

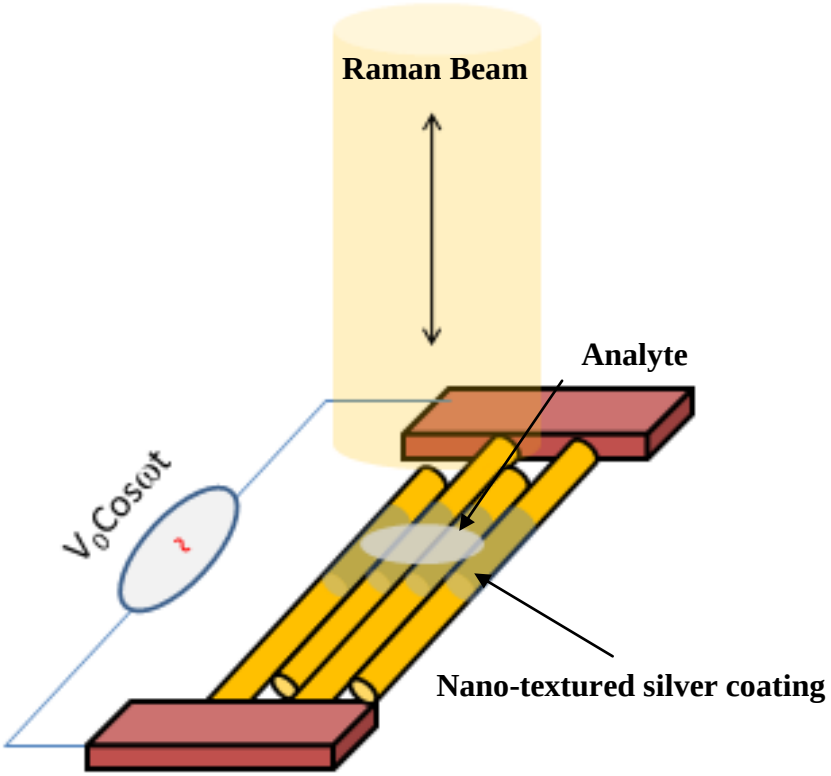

Figure 17: *Schematic diagram of interdigitated fiber optic strands with thin silver coating.*

Another concept that is still under investigation was based on the formation of nano-antenna structures with dimensions related to λ/4, where λ is the wavelength of the incident light. It is believed that with proper dimensional tuning, and suitable spacing between either a pair of such antenna or an array of such antennae, the SERS effect can be greatly increased, reproducibly. Preliminary work has begun to investigate these phenomena; however, the results are yet to be published. A diagrammatic representation of the antennae structures that are under investigation is shown in Figure 18. The structures were formed using an AFM tip over a 100nm silver coated Si wafer.

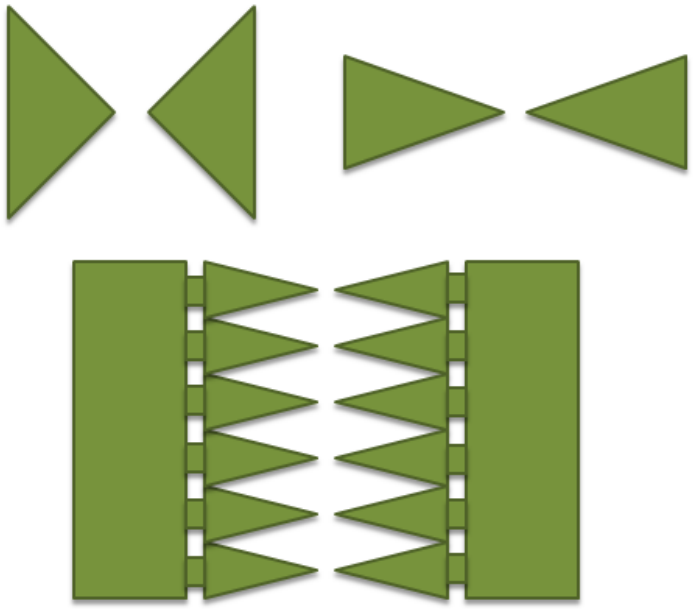

Figure 18: *Diagram showing different antenna structures designs to investigate the effect on SERS. Antenna with varying angles at apex, and also arrays of antennae are proposed for future study.*

Truly, there is plenty of room for more work in this field as the formation of DLA structures is very intricate and requires much attention. Research is currently being carried out to fashion a technique to create the fractal structures more conveniently. Once such a system is established, the areas of applications of this substrate are endless. Furthermore, the effect of E-field enhanced SERS is one that is suppliant for attention, but has not received much yet. The vision of achieving single molecule detection, such as in DNA base sequencing, is just a few steps away as individual bases are readily identifiable by its Raman spectrum [14].

C H A P T E R 5

CONCLUSION

This thesis has provided evidence of a new substrate that can be easily prepared and applied to SERS. Bearing in mind the other numerous methods that have been applied to obtain high SERS, such as electrochemically roughened gold electrodes, silver colloidal nanoparticles deposited on roughened silver surfaces or AgO films deposited on glass slides and microfabricated nano-structures coated with SERS active material (such as silver and/or gold), the method utilized here is unique in the way that it requires far less preparation time and effort. The creation of fractal geometric structures by Diffusion Limited Aggregation via the use of Dielectrophoresis results in formation of nanostructures, which, when used in conjunction with a simple Raman Spectrometer, can repeatedly result in high Raman signal enhancements ($\sim 10^9$) of analyte molecules, such as Thymine.

B I B L I O G R A P H Y

1. E. Smith and G. Dent, *Modern Raman Spectroscopy: A Practical Approach*. Chichester, West Sussex, England, John Wiley & Sons Ltd., 2005.

2. X. Jiang, L. Zhang, T. Wang and Q. Wan, "High surface-enhanced Raman scattering activity from Au-decorated individual and branched tin oxide nanowires," *Journal of Applied Physics* , vol. 106, no. 10, pp.104316-104316-5, Nov. 2009. .

3. M. S. Schmidt, A. Boisen and J. Hubner, "Towards easily reproducible nano-structured SERS substrates," *Sensors, 2009 IEEE* , pp. 1763-1767, Oct. 2009.

4. Y. Ghallab and W. Badawy, "Sensing methods for dielectrophoresis phenomenon: From bulky instruments to lab-on-a-chip," *Circuits and Systems Magazine, IEEE* , vol. 4, no. 3, pp. 5- 15, Third Quarter 2004.

5. T. A. Whitten and L. M. Sander, "Diffusion-limited aggregation, a kinetic critical phenomenon," *Phys. Rev. Lett.*, vol. 47, no. 19, pp. 1400-1403, Nov. 1981.

6. M. Kim, Y. Kim, E. Kuk, D. H. Jeong, K. Lee and C. Baek, "Controlled aggregation of silver nanoparticles using DEP force for SERS (surface enhanced Raman spectroscopy) analysis," *Solid-State Sensors, Actuators and Microsystems, 2005. Digest of Technical Papers. TRANSDUCERS '05. The 13th International Conference*, vol. 2, pp. 1768- 1771, June 2005.

7. A. C. Brieva, L. Alves, S. Krishnamurthy and L. Siller, "Gold surface with gold nitride–a surface enhanced Raman scattering active substrate," *Journal of Applied Physics* , vol. 105, no. 5, pp. 054302-054302-4, Mar. 2009. .

8. C. Otto, T. Tweel, F. Mul, and J. Greve, "Surface-enhanced Raman spectroscopy of DNA bases," *Journal of Raman Spectroscopy*, vol. 17, no. 3, pp. 289-298, 2005.

9. T. Ichimura, T. Suwa, Y. Otsuka, Y. Inouye, S. Kawata, H. Tabata and T. Kawai, "Detection and identification of DNA bases by tip enhanced Raman spectroscopy," *Quantum Electronics Conference, 2005. International* , pp. 1054- 1055, Jul. 2005.

10. X. Dong, H. Gu, J. Kang, J. Wu and X. Yuan, "Study on surface-enhanced raman scattering of phenylalanine using different aggregating agents for borohydride-reduced silver colloid," *Biomedical Engineering and Informatics, 2009. BMEI '09. 2nd International Conference*, pp. 1-4, Oct. 2009.

11. K. H. Bhatt and O. D. D. Velev, “Control and Modeling of the Dielectrophoretic Assembly of On-Chip Nanoparticle Wires,” *Langmuir*, vol. 20, no. 2, pp. 467-476, 2004.

12. E. C. Le Ru, P. G. Etchgoin, *Principles of Surface-Enhanced Raman Spectroscopy and Related Plasmonic Effects.* Amsterdam, Elsevier B. V., 2009.

13. D. Liu and S. V. Garimella, "Microfluidic pumping based on dielectrophoresis for thermal management of microelectronics," *Thermal and Thermomechanical Phenomena in Electronic Systems, 2008. ITHERM 2008. 11th Intersociety Conference*, pp.545-554, May 2008 .

14. H. A. Pohl, *Dielectrophoresis.* Cambridge, Cambridge University Press, 1978.